Article:
Ruiz-Perez, L., Madsen, J., Themistou, E. et al. (2015) Nanoscale detection of metal-labeled copolymers in patchy polymersomes. Polymer Chemistry, 6 (11). pp. 2065-2068. ISSN: 1759-9954

https://doi.org/10.1039/c4py01508h

Polymer Chemistry

Accepted Manuscript

ROYAL SOCIETY OF CHEMISTRY

www.rsc.org/polymers

Nanoscale detection of metal-labeled copolymers in patchy polymersomes

Lorena Ruiz-Pérez, [†,§,‡] Jeppe Madsen, [⊥,#,‡] Efrosyni Themistou, [⊥,¶,‡] Jens Gaitzsch, [†,§] Léa Messager, [†,§] Steven P. Armes, [⊥] Giuseppe Battaglia[*,†,§]

[†]Department of Chemistry and [§]The MRC/UCL Centre for Medical Molecular Virology, University College London, London, United Kingdom. [⊥]Department of Chemistry The University of Sheffield, Sheffield, United Kingdom

We report the synthesis of polymersome-forming block copolymers using two different synthetic routes based on Atom Transfer Radical Polymerization (ATRP) and Reversible Addition Fragmentation chain Transfer (RAFT) polymerization, respectively. Functionalization with 1,4,7,10-tetraazacyclododecane-1,4,7,10-tetraacetic acid (DOTA) allowed the block copolymer chains to be labelled with electron-dense metal ions (e.g. indium). The resulting metal-conjugated copolymers can be visualized by transmission electron microscopy with single chain resolution, hence enabling the study of polymer/polymer immiscibility and phase separation on the nano-scale.

Biological membranes are composed of several components whose two-dimensional arrangement is controlled by membrane-confined interaction. Depending on the chemical nature and composition, the various membrane components can segregate to form domains (a.k.a. 'rafts') ranging in size from tens to hundreds of nm. Such domains play an important role in cellular signaling, membrane trafficking and membrane modeling.[1, 2] Recently, this surface topological control has been reproduced using synthetic membrane-forming block copolymers, thus enabling the formation of vesicles (a.k.a. polymersomes),cylinders, and micelles with patterned surfaces.[3-11] In particular, we have observed that patchy polymersomes formed by cell-active and cell-inert chemistries can enter cells much more efficiently than comparable polymersomes with uniform surface chemistries.[3, 4] This suggests that controlling the topological arrangements of (polymeric) ligands on the surface of nanoparticles can enhance their interaction with cells that favor receptor clustering.

Controlled mixing of membrane-forming block copolymers leads to the formation of patchy polymersomes where the surface topology is controlled by the molar ratio of the block copolymer chains, as well as their molecular weight.[4] In the case of binary copolymer mixtures, patchy polymersomes can be formed by judicious mixing of diblock copolymers in three ways: (i) AB/CD, whereby phase separation is driven by chemically dissimilar hydrophobic *and* hydrophilic blocks; (ii) AB/CB, whereby phase separation is driven solely by chemically dissimilar *hydrophilic* blocks; (iii) AB/AD, whereby phase separation is driven solely by chemically dissimilar *hydrophobic* blocks.[4] In general, the patches are formed by the minor copolymer component in each case. Furthermore, it was found that, on ageing, the total number of domains on the polymersome surface decreased while their surface area increased until complete phase segregation occurred, leading to asymmetric polymersomes.[3, 4] In order to engineer polymersomes with a given surface topology, it is necessary to be able to assess the patch size and shape. Although this has been achieved, a significant amount of sample preparation and/or substantial mathematical manipulation of the acquired images were necessary to visualize (and hence quantify) the patches.[3, 4] In addition, the domains had to be relatively large to be detected, hence preventing studies of the onset of phase separation. Here, direct imaging of polymersome domains by transmission electron microscopy (TEM) and scanning transmission electron microscopy (STEM) is reported. This is facilitated by using a copolymer labeled with an electron-dense transition metal (Indium) as one of the components in the binary mixture. This metal and its associated copolymer can be visualized directly by transmission electron microscopy even in the absence of any additional staining.

To label polymersome-forming copolymers with heavy metals, we conjugated 1,4,7,10-tetraazacyclododecane-1,4,7,10-tetraacetic acid (DOTA). This is a well-established complexing agent for many metal ions and already used in several medical applications.[12] In our first approach we synthesized a DOTA labeled poly(2-(methacryloyloxy)ethyl phosphorylcholine)- poly(2-(diisopropylamino)ethyl methacrylate) (DOTA-PMPC-PDPA) block copolymer. The polymer was achieved using atom transfer radical

polymerization (ATRP, see SI), yielding an AB-SS-BA tetrablock as previously published by our group.[13] The disulfide bond was then cleaved and the resulting AB-SH thiols react with the maleimide fuctionalized DOTA, forming the final DOTA-PMPC-PDPA. This copolymer is subsequently incubated with $InCl_3$ to facilitate indium labeling, hence producing In-DOTA copolymer (**1**). The extent of indium labeling was determined using inductively coupled plasma (ICP) spectrometry to detect the metal cation. As shown in Fig S1, an indium content corresponding to more than one indium atom per copolymer chain was determined for the In-DOTA-PMPC-PDPA **(1)** indicating that the copolymer chains also bind to the metal. Further experiments using non-functionalised PMPC-PDPA, and other PDPA copolymer synthesised with different hydrophilic blocks: Poly(ethylene oxide) PEO and Poly(oligoethylene glycol methacrylate) (POEGMA) confirmed that this binding occurs with the PDPA chains. It is worth noting that even the addition of strong chelating agent Ethylenediaminetetraacetic acid (EDTA) did not remove the metals from the polymer. However further analysis using GPC and NMR gave no conclusive evidence of how and where the Indium is bound to the polymer (see SI), we can postulate that the amine groups of the DPA units act as chelating agents. Nevertheless, after switching to acidic conditions, only the DOTA labelled PMPC-PDPA was able to retain Indium, giving final proof that the metal ion is bound to its ligand and that we can label *ad hoc* specific polymer chains.

Scheme 1. Polymers used in this study. In-DOTA-$PMPC_{25}$-$PDPA_{70}$ (**1**) via ATRP and $PMPC_{18}$-stat-$DOTA_z$ macro-CTA (**2**) for the RAFT approach.

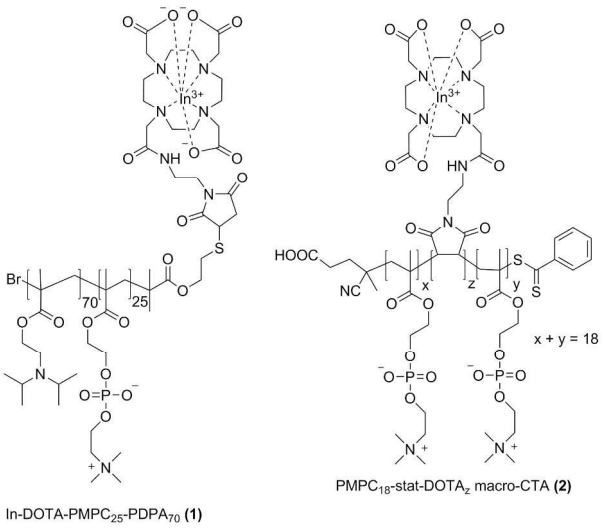

In-labeled PMPC-PDPA polymersomes were imaged using TEM and STEM. We confirmed the In labelling using Energy-dispersive X-ray spectroscopy (EDX). In fig. 1 a, the EDX spectrum shows the corresponding peak to the Indium and this signal has been mapped on the corresponding STEM micrograph (fig.1b). It is evident the majority of the Indium signal is localised onto the polymersome surface confirming the effective labelling is retained after polymersomes formation.

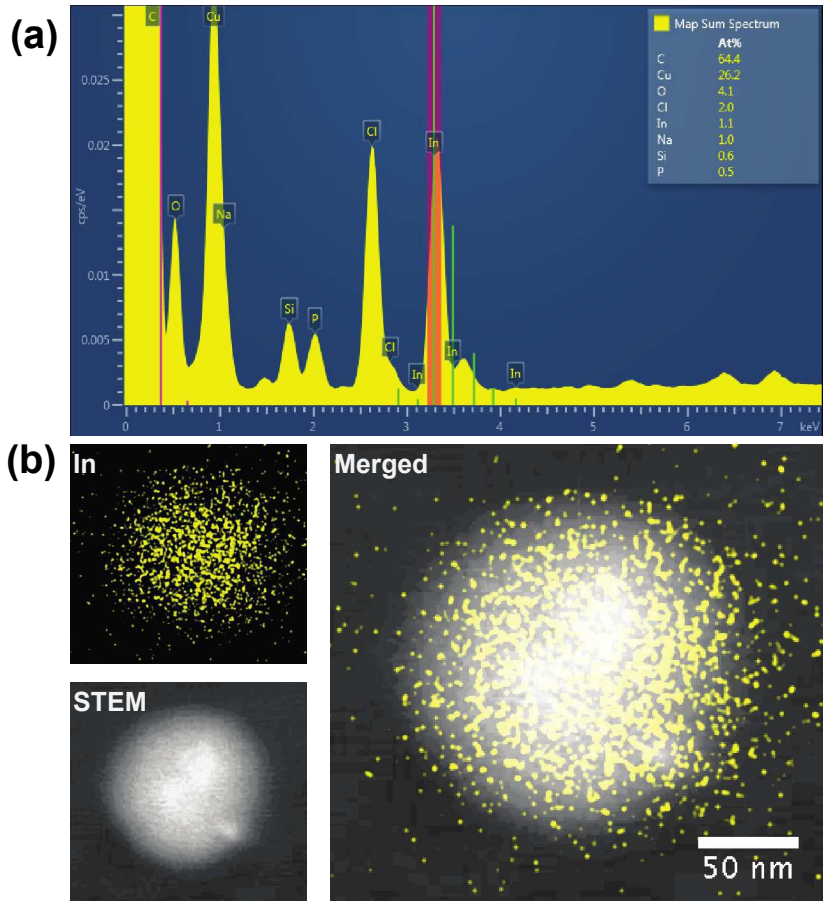

Figure.1 (a) EDX spectrum of In-PMPC-PDPA with elements atomic %, **(b)** layered In mapping+ electron images of In-PMPC-PDPA,

In-labeled DOTA-PMPC-PDPA diblock copolymers were mixed with PEO-PDPA diblock copolymers to form patchy polymersomes. These were prepared using a film hydration technique. In Figure 2a, the TEM image for a In-DOTA-PMPC-PDPA/PEO-PDPA (1:9 mol:mol) polymersome was recorded 14 days after preparation. Numerous dark circular domains randomly distributed on the polymersome surface can be observed directly on the native TEM picture, without any image processing being required. The molecular surface area of each PMPC chain at the PDPA membrane surface can be calculated by rearranging the packing parameter equation[7] as to $a_m = v_m/(pt)$. Where a_m is the optimal area per PMPC-PDPA copolymer chain, v_m is the PDPA molecular volume, p is the packing factor and t is the membrane thickness. While both v_m and t can be calculated (or measured), the packing factors for membrane-forming amphiphiles vary from 0.50 to 1.00, where unity is the theoretical limit for planar membranes.[7] In this case v_m was calculated assuming a PDPA density of 1 g cm^{-3}, and t was estimated from TEM images.

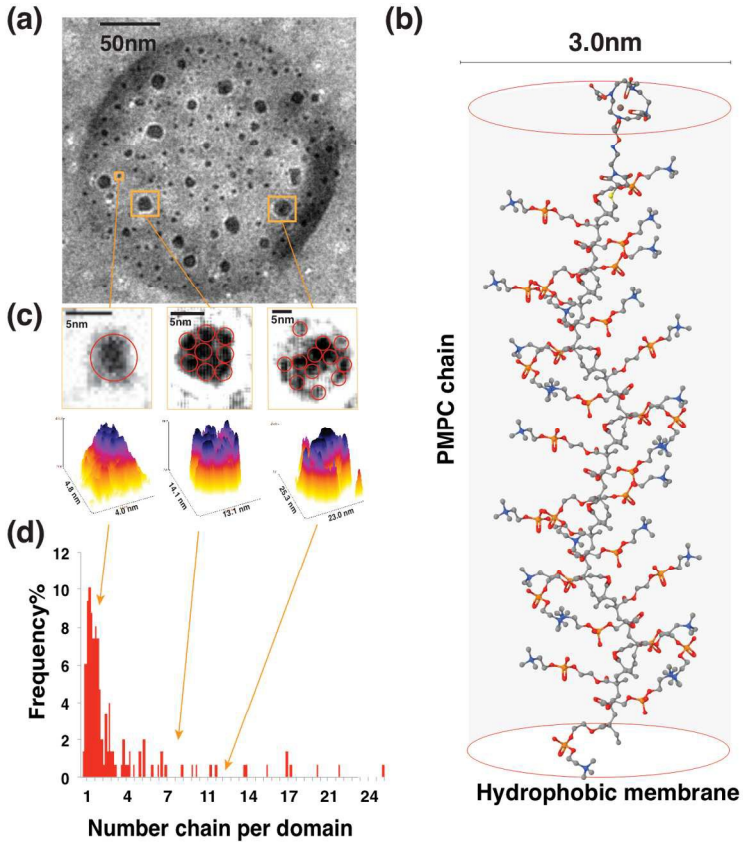

Figure 2. (a) TEM images obtained for a 1:9 mol: mol In-PMPC-PDPA/PEO-PPDPA polymersome. **(b)** Atomistic model of a single $PMPC_{25}$ chain stretching out from the hydrophobic polymersome membrane. **(c)** High magnification TEM showing different domains comprising 1, 7 and 12 PMPC chains. **(d)** Statistical distribution of the PMPC domains in term of number per chain per domain.

We have previously observed that, for $PMPC_{25}$-$PDPA_x$ copolymers, x = 70 is the minimum degree of polymerization of the PDPA block that gives polymersomes, whereas lower degree of polymersization favors micelle formation.[5]

Hence the packing factor for $PMPC_{25}$-$PDPA_{70}$ should be close to 0.50, which is the lower limit for vesicle formation. For p = 0.50, we calculate that the $PMPC_{25}$-$PDPA_{70}$ copolymers have an optimal area of 7.25 nm^2. This leads to an average separation distance between any two adjacent $PMPC_{25}$–$PDPA_{70}$ chains of about 1.5 nm, meaning that one chain covers an area with 3 nm in diameter. As demonstrated previously, the hydrophilic stabilizer block of polymersome-forming copolymers has a fully stretched conformation with its thickness being directly proportional to its degree of polymerisation.[8] Using a Merck Molecular Force Field algorithm[9] (MMFF94) for a $PMPC_4$ oligomer, we minimized its structure and formed a fully-stretched $PMPC_{25}$ chain by adding up the necessary number of oligomers. The resulting atomistic model is shown in Figure 2b, where it can be seen that the PMPC chain occupies a cylindrical volume with a diameter of about 3 nm. This is well in line with the area per molecule required to form a polymersome as discussed above. Figure 2c shows highly magnified images of three chosen domains with size corresponding to 1, 7 and 12 PMPC chains as shown by the superimposed red circle. The number of domains n per polymersome was found to be relatively large, ranging between 75 and 150. Statistical analysis of the number of patches and mean areas per patch was performed on five different polymersomes after 14 days of stirring at 20°C, as described in the experimental part in the supporting information. Probability distributions of domain area, number of PMPC molecules per domain and fractional area versus frequency of appearance for different polymersomes are shown in the supporting information (Fig. S4-S6). The number of PMPC chains per domain plotted against frequency density for a specific polymersome (1:9 molar ratios) with 150 patches (n = 150) is shown in Figure 2d. The TEM resolution achieved using indium-labeled copolymers is sufficient to image single chains. Most domains comprise just one PMPC chain, with larger domains generally being less

abundant. A single PMPC chain is of course simply in solution (i.e. it cannot be phase-segregated), hence Figure 2 represents the early stages of phase separation at the molecular level.

An alternative route for the synthesis of well-defined block copolymers is reversible addition–fragmentation chain transfer **(**RAFT) polymerization.[10]

We therefore also introduced DOTA labeling during the synthesis of a PMPC macromolecular chain transfer agent (macro-CTA) (Scheme 1, details in SI). MPC was polymerized in the presence of a small amount (targeting 1 per polymer chain, 1.38 achieved) of maleimidomonoamide-DOTA to produce the desired In-DOTA-PMPC macro-CTA (**2**). This In-labeled macro-CTA can then be used for the RAFT synthesis using 2-hydroxypropyl methacrylate (HPMA) under RAFT aqueous conditions. Such a formulation produces polymersomes via polymerization-induced self-assembly (PISA) in concentrated solution using a highly convenient one-pot protocol, as shown in our previous work.[11] In the present study, the In-DOTA-PMPC macro-CTA was mixed with a poly(ethylene oxide) (PEO) macro-CTA[12] (1:1 molar ratio) and the mixture was chain extended targetting the formation of 1:1 In-DOTA-PMPC-PHPMA/PEO-PHPMA polymersomes (Figure 3a). Again, the indium labeling allows visualization of the PMPC domains with single-chain resolution. In contrast to the polymersomes formed by thin film rehydration, the PISA method allows the preparation of hybrid polymersomes using perfectly mixed PMPC and PEO chains. The TEM images shown in Figure 3a were recorded for polymersomes immediately after PISA preparation, with domains containing just one or two PMPC chains per domain. This would suggest that the PEO and In-DOTA-PMPC macro-CTAs each polymerize HPMA at comparable rates, hence the final hybrid polymersome comprises a similar PMPC/PEO molar ratio to that initially targeted. Indeed, TEM analysis suggests that the In-labeled domains occupy a surface area of about 41 ± 12 % of the total polymersome – being in total unity with the initially targeted ratio.

Figure 3. TEM images obtained for 1:1 In-PMPC-PHPMA/PEO-PHPMA polymersomes at two different magnifications imaged 1 day (**a**), 30 days **(b**) and 60 days (**c**) after synthesis. The scale bar in the inset is 50

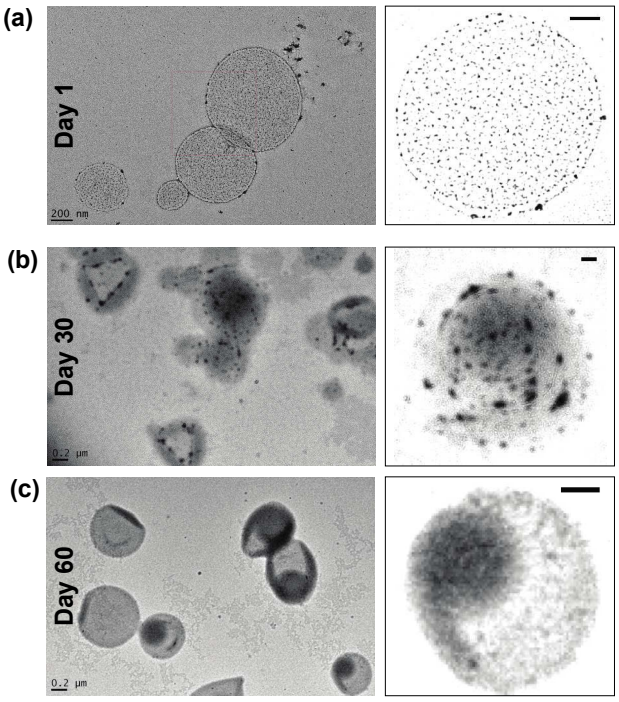

nm

As shown in Figure 3, we can now use this approach to monitor the ageing of the PMPC/PEO mixture. As expected, the de-mixing kinetics are rather slow and only after 60 days can one observe almost full separation (Figure 3c). This is because the membrane-forming PHPMA block has a relatively high molecular weight (38 kDa) and hence low lateral diffusion, as known for polymersomes.[14,13] Interestingly, in the present work we observed PMPC-PHPMA/PEO-PHPMA patterns that are more typical of bimodal decomposition (see Figure 3b). In our previous experiments, the copolymers were mixed in a 1:1 molar ratio in the solid state and then rehydrated in water. With such a protocol, we always observed a stripy pattern that is more typically characteristic of spinodal decomposition.[14] However, as shown in Figure 2a, such an approach fa-

vors the presence of clusters containing more than one chain that can act as nucleation site and hence drive faster de-mixing and therefore the formation of typical spinodal patterns. Finally, we can convert the pattern observed in the TEM images to more quantitative data by monitoring the degree of coarsening that occurs *en route* to fully phase-separated (see SI) (and consequently asymmetric, or Janus-like) polymersomes, as visualized in Figure 3c.

In summary, we report an effective way to introduce heavy metals into polymersome-forming diblock copolymers via two different methodologies. This enables electron microscopy imaging with unprecedented resolution and thus the visualization of nanoscale clustering formation at a molecular level. We also anticipate that both synthetic routes should allow the introduction of paramagnetic gadolinium, radioactive ions and other metals commonly used for either magnetic resonance imaging (MRI) of positron emission tomography (PET). If so, this would constitute an effective and reliable means of facilitating accurate pharmacokinetic studies of polymeric nanoparticles.

ASSOCIATED CONTENT

(**Supporting Information**. Experimental and materials, further data on TEM imaging, ICP indium labeling are included as Supporting Information. This material is available free of charge via the Internet at http://pubs.acs.org.

AUTHOR INFORMATION

Corresponding Author

Prof Giuseppe Battaglia, Dept of Chemistry, 20 Gordon Street, London, WC1H 0AJ, UK
email: g.battaglia@ucl.ac.uk T: +44 (0) 20 7679 4688

Present Addresses

¶School of Chemistry and Chemical Engineering, Queen's University Belfast, Belfast, BT9 5AG, UK

Author Contributions

‡These authors contributed equally

Funding Sources

This work was funded by the ERC (grant ERC-STG-MEVIC) and the EPSRC (grant EP/I001697/1).

Graphical abstract

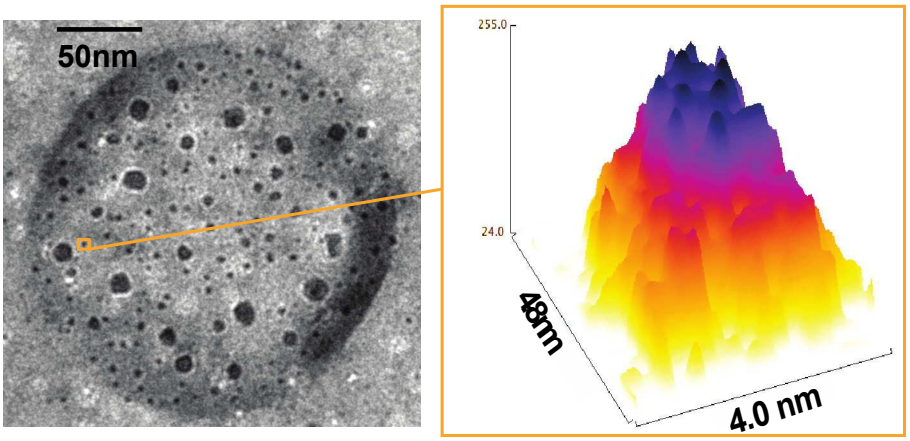

REFERENCES

1. K. Jacobson, O. G. Mouritsen and R. G. W. Anderson, *Nature Cell Biol.*, 2007, **9**, 7 - 14.

2. D. Lingwood and K. Simons, *Science*, 2010, **327**, 46-50.
3. M. Massignani, C. LoPresti, A. Blanazs, J. Madsen, S. P. Armes, A. L. Lewis and G. Battaglia, *Small*, 2009, **5**, 2424-2432.
4. C. LoPresti, M. Massignani, C. Fernyhough, A. Blanazs, A. J. Ryan, J. Madsen, N. J. Warren, S. P. Armes, A. L. Lewis, S. Chirasatitsin, A. J. Engler and G. Battaglia, *ACS Nano*, 2011, **5**, 1775-1784.
5. D. A. Christian, A. Tian, W. G. Ellenbroek, I. Levental, K. Rajagopal, P. A. Janmey, A. J. Liu, T. Baumgart and D. E. Discher, *Nat Mater*, 2009, **8**, 843-849.
6. G. Battaglia, C. LoPresti, M. Massignani, N. J. Warren, J. Madsen, S. Forster, C. Vasilev, J. K. Hobbs, S. P. Armes, S. Chirasatitsin and A. J. Engler, *Small*, 2011, **7**, 2010-2015.
7. A. H. W. Groschel, A.; Lobling, T. I.; Schacher, F. H.; Schmalz, H.; Muller, H. E, *Nature*, 2013, **503**, 247-251.
8. Z. H. Li, M. A.; Lodge, T. P., *Macromolecules*, 2006, **39**, 765-771.
9. Z. K. Li, E.; Talmon, Y.; Hillmyer, M. A.; Lodge, T.P, *Science*, 2004, **306**, 98-101.
10. D. J. Z. Pochan, J.; Zhang, K.; Wooley. K. L.; Miesch, C.;Emrick, T., *Soft Matter*, 2011, **7**, 2500-2506.
11. J. B. Nam, P. A; Vanderlick, T. K, *Langmuir*, 2011, **27**, 1-6.
12. H. Stetter and W. Frank, *Angewandte Chemie International Edition in English*, 1976, **15**, 686-686.
13. J. Madsen, S. P. Armes, K. Bertal, H. Lomas, S. Macneil and A. L. Lewis, *Biomacromolecules*, 2008, **9**, 2265-2275.
14. C. LoPresti, M. Massignani, C. Fernyhough, A. Blanazs, A. J. Ryan, J. Madsen, N. J. Warren, S. P. Armes, A. L. Lewis, S. Chirasatitsin, A. J. Engler and G. Battaglia, *ACS Nano*, 2011, **5**, 1775-1784.